Synthesis of borate-doped La10Ge6O27

thomas, samuel; James, Matthew; Stockham, Mark; jarvis, abbey; Slater, Peter

DOI:
10.1149/10301.1885ecst

Document Version
Peer reviewed version

Citation for published version (Harvard):
thomas, S, James, M, Stockham, M, jarvis, A & Slater, P 2021, 'Synthesis of borate-doped $La_{10}Ge_6O_{27}$: confirming the presence of a secondary conduction pathway', *ECS Transactions*, vol. 103, no. 1, pp. 1885-1897. https://doi.org/10.1149/10301.1885ecst

Synthesis of Borate-doped $La_{10}Ge_6O_{27}$: Confirming the Presence of a Secondary Conduction Pathway

Samuel W. Thomas, Matthew S. James*, Mark P. Stockham, Joshua Deakin, Abbey Jarvis, Peter R. Slater

School of Chemistry, University of Birmingham, Birmingham B15 2TT, United Kingdom

Abstract

The investigation of oxide ion conductivity in apatite germanates has attracted significant interest due to potential applications in SOFC electrolyte materials. These systems conduct via interstitial oxide ions, and a range of studies have indicated the importance of the GeO_4 units in the conduction process. In this paper, we investigate the effect of boron incorporation on the structure and conductivity. Studies show that heat treatment of $La_{10}Ge_6O_{27}$ with H_3BO_3 leads to an expansion in cell volume, attributed to incorporation of borate groups in the oxygen ion channels within the structure. For low levels of dopant i.e $La_{10}Ge_6O_{27}(BO_{1.5})_{0.5}$, a small enhancement in conductivity was observed attributed to a transition from a triclinic to a hexagonal apatite. For further increases in boron content, the conductivity was shown to decrease attributed to the blocking of the conduction pathway down the apatite channels. Interestingly, significant oxide ion conductivity was still observed, which provides the first experimental support for a secondary conduction mechanism perpendicular to the apatite channels proposed by prior modelling studies.

Introduction

The development of new materials for use in solid oxide fuel cells (SOFCs) has attracted considerable interest, with a view to improving their performance and lowering their operating temperature. Traditionally SOFC electrolyte work has focused on perovskite and fluorite systems, in which enhanced conductivity is observed through doping to introduce oxide ion vacancies (1, 2). Recently, however, there has been growing interest in alternative structure types, where interstitial oxide ions are the key defect. In this respect, apatite-type rare earth silicates and germanates have attracted particular interest (3-60). In these interstitial oxide ion conductors, the complexity of the conduction mechanism has made detailed understanding non-trivial, and a range of studies have attempted to clarify the conduction pathways (10, 16, 20).

In terms of these materials, the ideal apatite stoichiometry can be written as $A_{10}(MO_4)_6O_2$ (A = rare earth/alkaline earth; M = Ge, Si), and their structure can be viewed as an $A_4(MO_4)_6$ framework (consisting of corner linked MO_4 tetrahedra and AO_6 trigonal metaprisms), with the remaining A_6O_2 units within the "channel" of this framework (figure 1) (23, 24). The variation in the size of the A_6O_2 "channels" can be correlated with variations in the AO_6 metaprism twist angle (23). It has been reported that the apatite structure can accommodate excess interstitial oxide ions, which

contribute to the high conductivity of these systems. Different locations for these interstitial sites have been proposed, particularly for the apatite silicates, with most proposing a site close to the channel centre (7, 38, 39, 46).

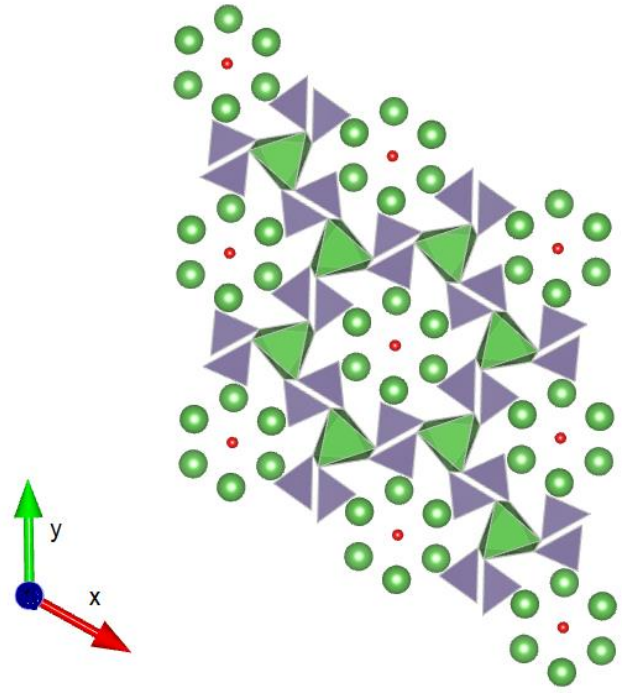

Figure 1: A visualisation of the $A_{10}(MO_4)_6O_2$ apatite structure (Space Group *P6₃/m*) with A_6O_2 units filling the channels within the $A_4(MO_4)_6$ framework.

For the apatite germanates, there is more general consensus that the interstitial oxide ions, that are responsible for the high conductivity, are located neighbouring the GeO_4 tetrahedra, converting some of these into GeO_5 units (24, 25, 40, 43, 49, 50, 61, 62).

An interesting recent observation in phosphate apatite systems is the potential for the incorporation of borate groups into the channels, with some reports claiming linear BO_2^- units (63, 64). We have therefore examined the possabillity that borate can be accommodated into the channel sites of the silicate/germanate apatite systems. Preliminary studies on the silicate systems suggested a reduction in cell volume consistent with partial substitution of silicate by borate as shown previously (65, 66). In contrast a reaction of apatite germanates with either B_2O_3 or H_3BO_3 shows an expansion in unit cell volume consistent with borate incorporation into a new site. In this paper, we report the effect on the structure and conductivity of this borate incorporation. Providing evidence for the first time of a secondary oxide ion conduction pathway.

Experimental

Samples were synthesised via a Pechini Method. Stoichiometric amounts of $La(NO_3)_3$, $Y(NO_3)_3$, and GeO_2 were all dissolved in deionised water whilst heating (100 ºC) and stirring. Citric Acid and Ethylene Glycol were added in the ratio 1:1:3 (Metal content : Ethylene Glycol: Citric Acid) and left to stir under heating for roughly 3 hours until a gel formed. The samples were then heated at 350 ºC (1 ºC min^{-1}) for 1 hour to burn off the organics. The resulting precursors were ground and the required stoichiometric amount of H_3BO_3 added, before heating at 700 ºC for 2 hours, regrinding, and reheating at 950 ºC for 12 hours. The powders were then pressed into pellets before a final heat treatment at 1100 °C for 4 hours.

Powder X-Ray diffraction data were collected to determine lattice parameters and phase purity of all samples. Data was collected on a Panalytical Empyrean diffractometer equipped with the Pixcel 2D detector (Cu Kα radiation). The GSAS-II suite of programs was used to determine unit cell parameters (67).

FT-IR Spectroscopy measurements were carried out to confirm the presence of borate. The measurements were collected on a Bruker Alpha II FTIR-Spectrometer with the platinum ATR attachment.

For conductivity measurements, the sintered pellets were coated with platinum paste on either side, platinum electrodes were attached to both faces, and the samples were heated at 950 ºC for 1 hour to ensure bonding to the pellet. The conductivities were then measured in a temperature range of 400 ºC to 800 ºC by AC impedance measurements (Hewlett Packard 4192A impedance analyser) in the range 0.1 to 10^3 kHz with an AC signal amplitude of 100 mV.

Results and Discussion

B doped $La_{10}Ge_6O_{27}$

Powder X-ray diffraction data for undoped $La_{10}Ge_6O_{27}$ indicated the formation of triclinic apatite with the space group *P -1* consistent with previous literature (23,24), see figure 2.

The synthesis of $La_{10}Ge_6O_{27}(BO_{1.5})_x$ (for x= 0.5, 1.0 and 1.5) was also performed, and in each case the formation of a hexagonal apatite (*P 6₃ / m*) phase was observed according to the powder X-ray diffraction data, with evidence for significant peak shifts with increasing B content, see figure 2

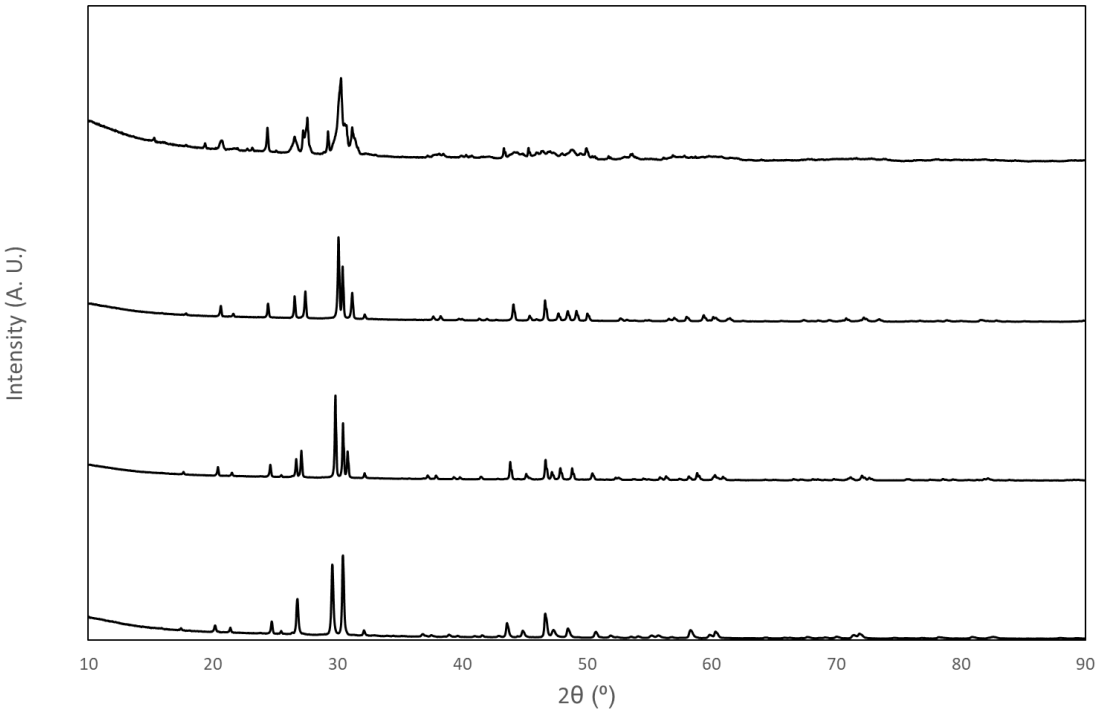

Figure 2: Powder X-ray Diffraction data for (from to top to bottom) $La_{10}Ge_6O_{27,}$ $La_{10}Ge_6O_{27}(BO_{1.5})_{0.5}$, $La_{10}Ge_6O_{27}(BO_{1.5})_{1.0,}$ $La_{10}Ge_6O_{27}(BO_{1.5})_{1.5}$ showing a triclinic cell for $La_{10}Ge_6O_{27}$ and a hexagonal cell with significant peak shifts for the B doped samples.

For the B doped samples, a structural model based on an apatite *P 6₃ / m* cell was successfully refined using the GSAS II suite of programs. The unit cell parameters from the refinements are shown in Table I. The unit cell volume was found to show a significant increase with increasing borate content. This differs to previous work where B was doped into the silicate apatites $La_{10-x}Si_6O_{27-3x/2}$, where a decrease in cell parameters was observed. For the silicate apatites, this could be explained by the substitution of smaller B in place of Si, with incorporation of up to 2 B possible to give $La_{10}Si_4B_2O_{26}$ (65). The increased cell volume for the Ge apatites is therefore of interest, as one might expect an even larger cell volume reduction, as B is much smaller than Ge. This indicates that B is not substituting in place of Ge, and rather B must be occupying a different site. Of relevance to this is the fact that it is known from previous studies that filling of the apatite channels tends to lead to an expansion along *a,b* and contraction along *c*, the former allowing for space for extra anions to be accommodated

without too short O-O interactions (68). Thus, the cell parameter changes suggest further filling of the channel sites, which we propose is due to incorporation of borate groups into these channels similar to such inclusion in phosphate apatites (63, 64). To support this assertation, attempts to prepare $La_{10}Ge_{6-x}B_xO_{27-x/2}$ samples (B substituted in place of Ge) were undertaken and these indicated very limited B incorporation. Furthermore, pre-preparing $La_{10}Ge_6O_{27}$ and reacting with different amounts of H_3BO_3 at 900 ^oC gave similar cell volume expansions as observed here/ supporting the incorporation of borate into new sites, i.e the apatite channels, within the structure.

Table I: Cell parameters and goodness of fit values for $La_{10}Ge_6O_{27}(BO_{1.5})_x$

x	a (Å)	c (Å)	Unit Cell Volume (Å^3)	$_wRp$	Rp	χ^2
0.50	9.9320(4)	7.2820(7)	622.103	5.53	1.89	2.92
1.00	10.0466(7)	7.2314(6)	632.122	5.97	1.88	3.18
1.50	10.1509(9)	7.1948(4)	642.049	6.55	1.93	3.48

When comparing the cell volumes of the $La_{10}Ge_6O_{27}(BO_{1.5})_x$ series, a linear increase with increasing borate concentration ($0.5 \leq x \leq 1.5$) is observed, attributed to the incorporation of borate within the channel, Figure 3. There is some deviation at x=0, which may be related to the change in cell symmetry (x=0, triclinic; $x \geq 0.5$ hexagonal) or may indicate a low level of B substitution for the GeO_4 site initially.

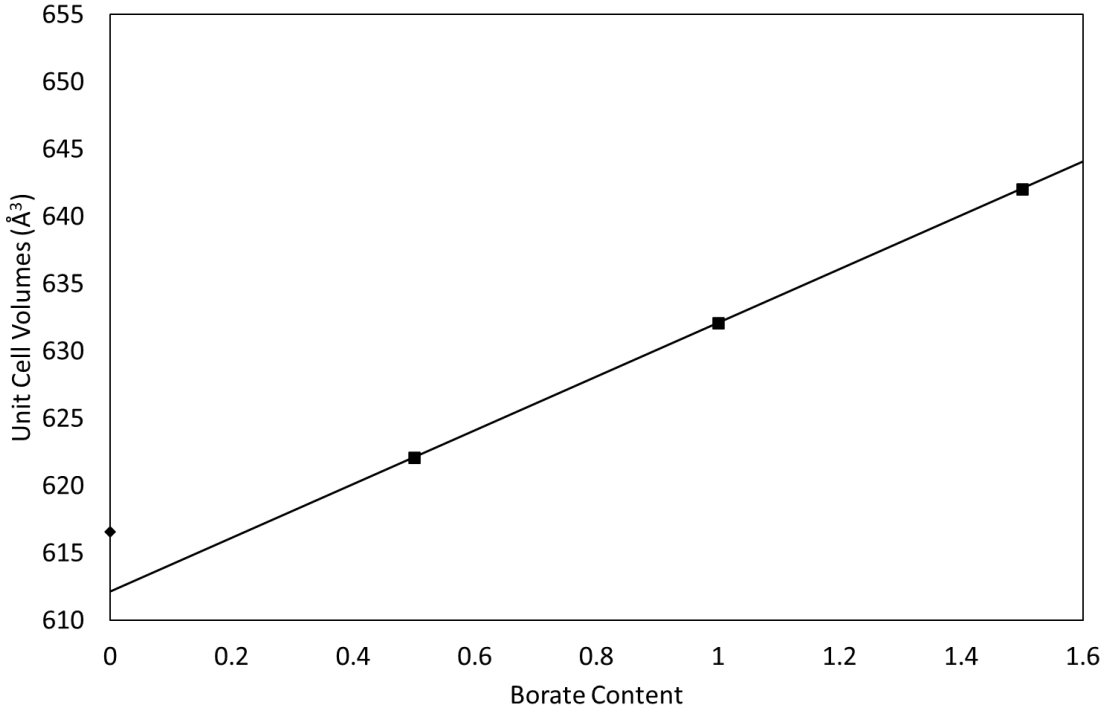

Figure 3: Unit Cell Volumes vs Borate content for $La_{10}Ge_6O_{27}(BO_{1.5})_x$

FT-IR spectra analysis was used to gather more information regarding the borate group within the apatite structure. Peaks attributed to borate were observed in the regions 860-920, 920-1000 and 1200-1400 cm^{-1}. Borate peaks in the regions of 860-920 and 920-1000 cm^{-1} can be attributed to BO_4 units whilst peaks in the region 1280-1350 cm^{-1} are usually assigned to a BO_3 unit. (69) The undoped material was observed to have no peaks present in these regions, with low level borate material showing the 860-920 and 920-1000 cm^{-1} peaks, while only the highest borate containing materials, $La_{10}Ge_6O_{27}(BO_{1.5})_{1.0}$ and $La_{10}Ge_6O_{27}(BO_{1.5})_{1.5}$ showed 1200-1400 cm^{-1} bands present, Figure 4.

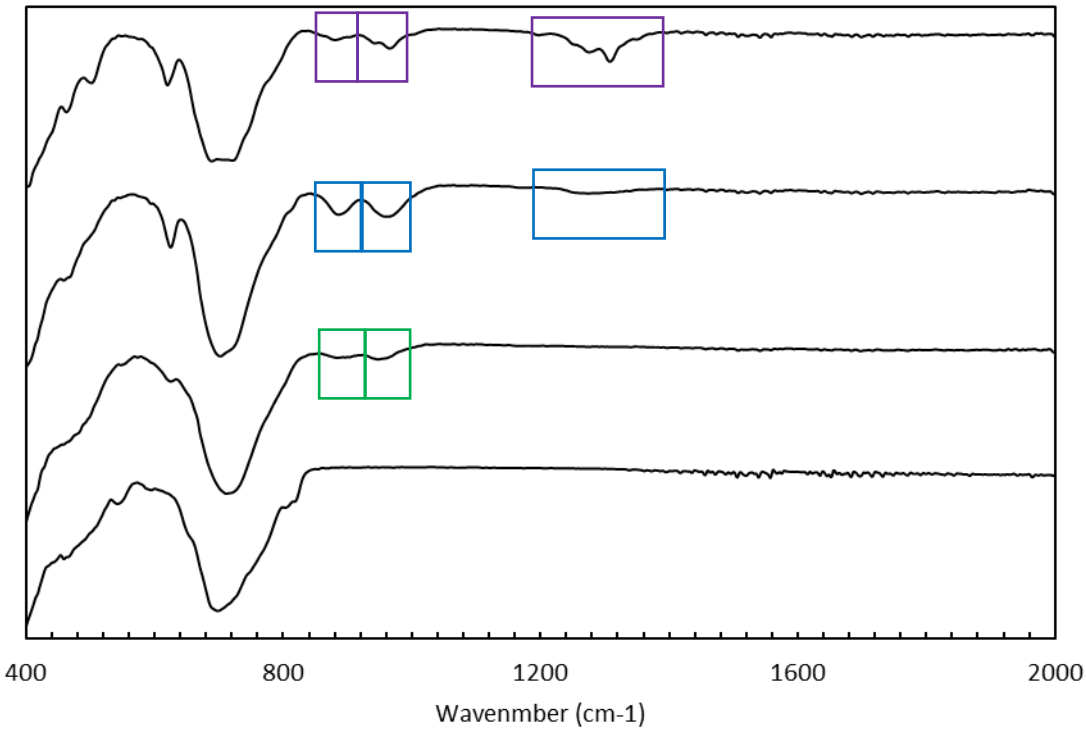

Figure 4: IR Spectra from top to bottom: $La_{10}Ge_6O_{27}(BO_{1.5})_{1.5}$, $La_{10}Ge_6O_{27}(BO_{1.5})_{1.0}$, $La_{10}Ge_6O_{27}(BO_{1.5})_{0.5}$ and $La_{10}Ge_6O_{27}$; data show the presence of 3 borate band regions.

The conductivity data for all samples are shown in Figure 5. These data show that there is an initial increase in conductivity on borate doping for x=0.5. This increase in conductivity can be attributed to a change in cell symmetry from triclinic (undoped) to hexagonal (doped), as seen for other doping strategies (12, 16, 21, 35). This appears to outweigh any negative consequence of borate blocking the apatite channels at this doping level.

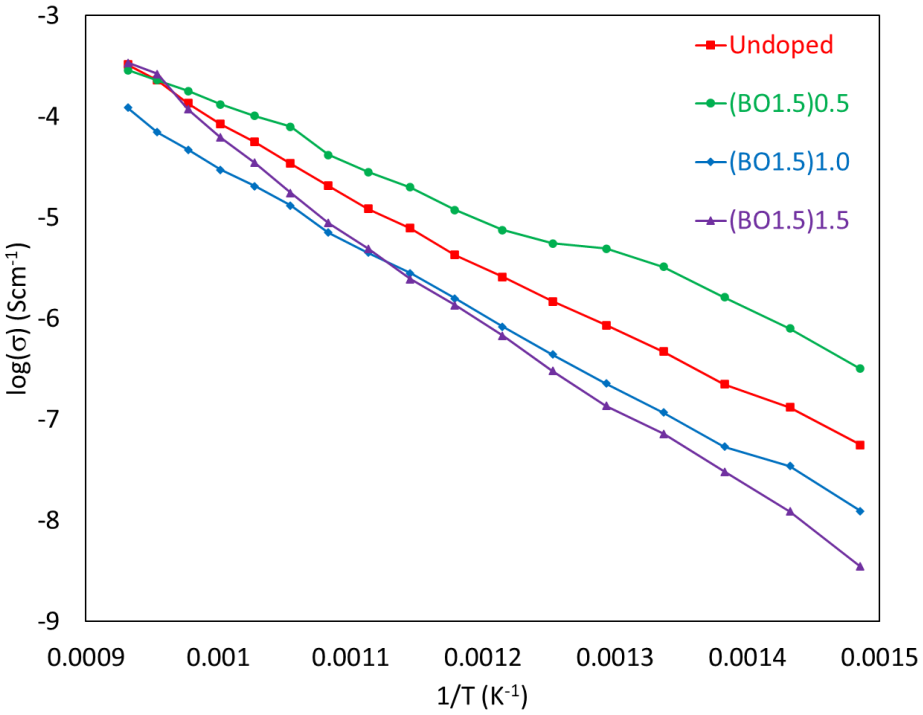

Figure 5: Plot of log σ versus 1/T for $La_{10}Ge_6O_{27}$ and $La_{10}Ge_6O_{27}(BO_{1.5})_x$

With increased dopant levels, i.e. $La_{10}Ge_6O_{27}(BO_{1.5})_{1.0}$ and $La_{10}Ge_6O_{27}(BO_{1.5})_{1.5}$, a decrease in conductivity is observed compared to the undoped $La_{10}Ge_6O_{27}$ sample at low temperatures. We attribute this decrease to increasing blockage of the central channel by the inclusion of borate and thus a loss of the *c*-direction oxide interstitial conduction mechanism. However, the most interesting observation is that substantial oxide ion conductivity still occurs suggesting that a secondary conduction mechanism is still present. This has not been experimentally reported prior, however has been suggested via computer modelling studies. These studies have proposed a conduction mechanism perpendicular to the channels, via a SN2 type mechanism (49), and so this work adds support for this mechanism.

At higher temperature $La_{10}Ge_6O_{27}(BO_{1.5})_{1.5}$ shows a rapid increase in conductivity comparable to the x=0.5 and undoped sample, which warrants further study, but may involve some sort of cooperative mechanism involving the borate groups.

Conclusion

In this paper we have shown that borate can be incorporated within $La_{10}Ge_6O_{27}$ resulting in the synthesis of the hexagonal apatite series, $La_{10}Ge_6O_{27}(BO_{1.5})_x$ ($0.5 \leq x \leq 1.5$). The presence of this borate is confirmed by IR (peaks in the regions 860-920, 920-1000 and 1200-1400 cm^{-1}), and we propose that the borate is accommodated within the apatite channels in line with the observed increase in cell volume.

Conductivity measurements showed there was a general improvement for $La_{10}Ge_6O_{27}(BO_{1.5})_x$ materials for low levels ($x=0.5$) of borate incorporation, with a decrease in conductivity with higher concentration of borate ($x \geq 1$). Nevertheless, all samples show high levels of oxide ion conductivity despite the postulated inclusion of borate within the apatite channels (the main conduction pathway proposed for apatite materials). This would therefore support the existence of a second pathway perpendicular to the channels, as proposed by prior modelling studies.

Acknowledgement

The authors would like to thank the EPSRC (EP/R023662/1; The JUICED Hub [Joint University Industry Consortium for Energy (Materials) and Devices Hub]), as well as the Leverhulme Trust (RPG-2017-011) for funding. The raw datasets associated with the results in this paper are available form the University of Birmingham archive; https://doi.org/10.25500/edata.bham.00000683

References

1. A. Orera and P. R. Slater, *Chem. Mater.*, **22**, 675 (2010)

2. A. J. Jacobson, *Chem. Mater.,* **22**, 660 (2010)

3. S. Nakayama, H. Aono, Y. Sadaoka, *Chem. Lett.* **24**, 431-432 (1995)

4. S. Nakayama, M. Sakamoto, M. Higuchi, K. Kodaira, *J. Mater. Sci. Lett*. **19,** 91-93 (2000)

5. H. Arikawa, H. Nishiguchi, T. Ishihara, Y. Takita, *Solid State Ionics* **136-137,** 31-37 (2000)

6. S. Tao, J.T.S. Irvine, *Mater. Res. Bull.* **36**, 1245-1248 (2001)

7. J.E.H. Sansom, D. Richings, P.R. Slater, *Solid State Ionics* **139,** 205 (2001)

8. L. Leon-Reina, M.E. Martin-Sedeno, E.R. Losilla, A. Caberza, M. Martinez-Lara, S. Bruque, F.M.B. Marques, D.V. Sheptvakov, M.A.G. Aranda, *Chem. Mater*. **15,** 2099-2108 (2003)

9. E. J. Abram, C. A. Kirk, D. C. Sinclair, A.R. West, *Solid State Ionics* **176**, 1941-1947 (2005)

10. J. R. Tolchard, P. R. Slater, M. S. Islam, *Adv. Funct. Mater.* **17,** 2564-2571 (2007)

11. J. R. Tolchard, M.S. Islam, P. R. Slater, *J. Mater. Chem*. **13,** 1956-1961 (2003)

12. L. Leon-Reina, E.R. Losilla, M. Martinez-Lara, M.C. Martin-Sedeno, S. Bruque, P.Nunez, D.V. Sheptyakov, M.A.G. Aranda; *Chem. Mater*. **17,** 596-600 (2005)

13. L. Leon-Reina, E.R. Losilla, M. Martinez-Lara, S. Bruque, A. Llobet, D.V. Sheptyakov, M.A.G. Aranda, *J. Mater. Chem.* **15**, 2489-2498 (2005)

14. V.V. Kharton, A.L. Shaula, M.V. Patrakeev, J.C. Waerenborgh, D.P. Rojas, N.P. Vyshatko, E.V. Tsipis, A.A. Yaremchenko, F.M.B. Marques, *J. Electrochem. Soc*. **151,** A1236 (2004)

15. J.E.H. Sansom, J.R. Tolchard, D. Apperley, M.S. Islam, P.R. Slater, *J. Mater. Chem.* **16,** 1410-1413 (2006)

16. E. Kendrick, M.S. Islam, P.R. Slater, *J. Mater. Chem*. **17,** 3104-3111 (2007)

17. Y. Masubuchi, M. Higuchi, S. Kikkawa, K. Kodaira, S. Nakayama, *Solid State Ionics* **175**, 357-360 (2004**)**

18. S. Celerier, C. Laberty-Robert, J.W. Long, K.A. Pettigrew, R.M. Stroud, D.R. Rolison, F. Ansart, P. Stevens, *Adv. Mater*. **18,** 615-618 (2006**)**

19. L. Leon-Reina, J.M. Porras-Vasquez, E.R. Losilla, M.A.G. Aranda, *J. Solid State Chem.,* **180,** 1250-1258 (2007)

20. E. Kendrick, J.R.Tolchard, J.E.H. Sansom, M.S. Islam, P.R. Slater; *Faraday Discussions*., **134,** 181-194 (2007)

21. E. Kendrick, P.R. Slater, *Mater. Res. Bull*., **43,** 1913-2516 (2008)

22. E. Kendrick, P.R. Slater, *Mater. Res. Bull*., **43,** 3179-3634 (2008)

23. S. S. Pramana, W.T. Klooster and T. J. White, *Acta Cryst*. **B63,** 597-602 (2007)

24. S.S. Pramana, W.T. Klooster, T.J. White, *J. Solid State Chem*., **181,** 1717-1722 (2008)

25. E. Kendrick, M.S. Islam, P.R. Slater, *Chem. Commun*. 715-717 (2008)

26. A. Orera, E. Kendrick, D. C. Apperley, V.M. Orera, P.R. Slater, *Dalton Trans*. 5296-5301 (2008)

27. E. Kendrick, P.R. Slater; *Solid State Ionics* **179,** 981-984 (2008)

28. P.J. Panteix, I. Julien, P. Abelard, D. Bernache-Assolant,*Ceram. Int*., **34,** 1579-1586 (2008)

29. T. Iwata, K. Fukuda, E. Bechade, O. Masson, I. Julien, E. Champion, P. Thomas, *Solid State Ionics* **178,** 1523 (2008)

30. R. Ali, M. Yashima, Y. Matsushita, H. Yoshioka, K. Okoyama, F. Izumi, *Chem. Mater.* **20**, 5203-5208 (2008)

31. J.R. Tolchard, P.R. Slater, *J. Phys. Chem. Solids*, **69,** 2433-2439 (2008).

32. E. Kendrick, P.R. Slater, *Mater. Res. Bull*., **43,** 3627-3632 (2008)

33. A. Orera, P.R. Slater, *Solid State Ionics* **181,** 110-114

34. E. Kendrick, K.S. Knight, P.R. Slater; *Mater. Res. Bull*. **44** (2009) 1806.

35. J.M. Porras-Vazquez, E.R. Losilla, L. Leon-Reina, D. Marrero-Lopez, M.A.G. Aranda, *J. Am. Ceram. Soc*. **92,** 1062-1068. (2009)

36. C. Bonhomme, S. Beaudet-Savignat, T. Chartier, P-M. Geffroy, A-L. Sauvet, *J. Euro. Ceram. Soc.* **29,** 1781-1788 (2009)

37. A. Al-Yasari, A. Jones, D.C. Apperley, D. Driscoll, M.S. Islam, P.R. Slater, *J. Mater. Chem.* **19,** 5003-5008 (2009)

38. E. Bechade, O. Masson, T. Iwata, I. Julien, K. Fukuda, P. Thomas, E. Champion, *Chem. Mater*. 21, 2508-2517 (2009)

39. S. Guillot, S. Beaudet-Savignat, S. Lambert, R-N. Vannier, P. Roussel, F. Porcher, *J. Solid State Chem.,* **182,** 3358-3364 (2009)

40. E. Kendrick, A. Orera, P.R. Slater, *J. Mater. Chem.*, **19,** (2009) 7955-7958

41. A. Orera, D. Headspith, D.C. Apperley, M.G. Francesconi, P.R. Slater, *J. Solid State Chem.* **182** 3294-398 (2009)

42. T.J. White and Z.L. Dong, *Acta Crystallogr*., **B59,** 1-16 (2003)

43. A. Orera, M. L. Sanjuán, E. Kendrick, V. M. Orera, P.R. Slater; *J. Mater. Chem*., **20,** 2170-2175 (2010)

44. K. Fukuda, T. Asaka, M. Oyabu, D. Urushihara, A. Berghout, E. Bechade, O. Masson, I. Julien, P. Thomas, *Chem. Mater*., **24,** 4623-4631 (2012)

45. K. Fukuda, T. Asaka, N. Ishizawa, H. Mino, D. Urushihara, A. Berghout, E. Bechade, O. Masson, I. Julien, P. Thomas; *Chem. Mater*., **24,** 2611-2618 (2012)

46. K. Matsunaga, K. Toyoura; *J. Mater. Chem*., **22,** 7265-7273 (2012)

47. H. Kiyono, Y. Matsuda, T. Shimada, M. Ando, I. Oikawa, H. Maekawa, S. Nakayama, S. Ohki, M. Tansho, T. Shimizu, P. Florian, D. Massiot. *Solid State Ionics* **228,** 1-84 (2012)

48. K. Fukuda, T. Asaka, R. Hamaguchi, T. Suzuki, H. Oka, A. Berghout, E. Bechade, O. Masson, I. Julien, E. Champion, P. Thomas; *Chem. Mater*. **23**, 5474-5483 **(2011)**

49. P. M. Panchmatia, A. Orera, G. J. Rees, M. E. Smith, J. V. Hanna, P. R. Slater, M. S. Islam; *Angew. Chemie* **50,** 9328.-9333 (2011)

50. A. Orera, T. Baikie, E. Kendrick, J.F. Shin, S. Pramana, R. Smith, T. J. White, M.L. Sanjuán, and P.R. Slater; *Dalton Trans*. **40,** 3903-3908 (2011)

51. T. An, T. Baikie, F. Wei, S. S. Pramana, M. K. Schreyer, R. O. Piltz, J. F. Shin, J. Wei, P. R. Slater, and T. J. White; *Chem. Mater*. **25**, 1109-1120 (2013)

52. S. Nakayama, Y. Higuchi, M. Sugawara, A. Makiya, K. Uematsu, M. Sakamoto, *Ceramics Int*. **40,** 1221-1224 (2014)

53. G. Ou, X.R. Ren, L. Yao, H. Nishijima, W. Pan, *J. Mater. Chem. A* **2** 13817-13821 (2014)

54. H. Yoshioka, H. Mieda, T. Funahashi, A. Mineshige, T. Yazawa, R. Mori, *J. Euro. Ceram Soc.* 34 373-379 (2014)

55. W. Liu, T. Tsuchiya, S. Miyoshi, S. Yamaguchi, K. Kobayashi, W. Pan, *J. Power Sources* **248,** 685-689 (2014)

56. C. Argirusis, E. Jothinathan, G. Sourkouni, O. Van der Biest, F. Jomard, *Solid State Ionics* **257**, 53-59 (2014)

57. M.M. Vieira, J.C. Oliveira, A.L. Shaula, B. Trindade, A. Cavaleiro, *Surface and Coatings Technology*, **247,** 14-19 (2014)

58. A. Pons, J. Jouin, E. Bechade, I. Juilien, O. Masson, P.M. Geffroy, R. Mayet, P. Thomas, K. Fukuda, I. Kagomiya. *Solid State Sciences* **38,** 150-155 (2014)

59. T. An, T. Baikie, M. Weyland, J. Shin, P. Slater, J. Wei, T. White, *Chem. Mater*, **27,** 1217-1222 (2015)

60. T. An, A. Orera, T. Baikie, J. S. Herrin, R. O. Piltz, P. R. Slater, T. J. White, M. L. Sanjuán; *Inorg. Chem*. **53**, 9416-9423 (2014)

61. M. S. Chambers, P. Chater, I. R. Evans and J. S. Evans, *Inorg. Chem.,* **58**, 14853-14862 (2019).

62. K. Kobayashi, Y. Igarashi, N. Saito, T. Higuchi, Y. Sakka and T. S. Suzuki, *J. Ceram. Soc. Jpn.*, **126**, 91-98 (2018).

63. R. Ternane, M Cohen-Adad, G Panczer, C. Goutaudier, N. Kbir-Ariguib, M. Trabelsi-Ayedi, P. Florian, D. Massiot, *J. Alloys. Compd.* **333**, 62-71 (2002)

64. S. Barheine, S. Hayakawa, C. Jager, Y. Shirosaki, A. Osaka, *J. Am. Ceram. Soc.*, **94** (8) 2656-2662 (2011)

65.A. Najib, J.E.H Sansom, J.R Tolchard, P.R. Slater, M.S. Islam, *Dalton Trans.*, 3106-3109, (2004)

66. S. Ide, H, Takahashi, I. Yashima, K. Suematsu, K. Watanabe, K. Shimanoe, J. Phys. Chem. C., **124**(5), 2879-2885 (2020)

67. B. H Toby, R. B. Von Dreele, *J. Appl. Crystallogr*, **46**, 544-549 (2013).

68. B. J. Corrie, J.F. Shin, S. Hull, K.S Knight, M.C Vlachou, J.V. Hanna, P.R. Slater *Dalton Trans.*, **45**, 121-133 (2016)

69. C. E. Weir and R. A. Schroeder, *J. Res Natl Bur Stand A Phys Chem.*, **68A**, 465-487 (1964)